

# Practical Implications of Recent Cross-Eye Jamming Research

Warren P. du Plessis

Council for Scientific and Industrial Research (CSIR), Pretoria, 0001, South Africa

**Abstract**—Research into retrodirective cross-eye jamming has been conducted at the CSIR since 2007. The main results of this research are summarised in this paper, including the fact that a retrodirective cross-eye jammer can break a monopulse radar lock. The effect of system tolerances and platform skin return have also been quantified, and the construction of an operational system has been shown to be less challenging than is usually assumed. A simple cross-eye laboratory demonstrator was constructed using in-house DRFM technology and was successfully tested against a monopulse radar.

**Keywords**—Cross-eye jamming, electronic warfare (EW), electronic countermeasures (ECM), and electronic attack (EA).

## I. INTRODUCTION

Cross-eye jamming is an extremely old idea with two patents describing the concept being filed in 1958 (though they were only issued in the late 1970s) [1], [2]. Despite its age, cross-eye jamming has remained of interest to the electronic warfare (EW) community and is described in essentially every book on EW (e.g. [3]–[9]) and many books on radar (e.g. [10]–[15]).

The main reason for this sustained interest in cross-eye is that it is one of only a very small number of viable countermeasures to monopulse radar seekers [6], [15]–[18]. However, the challenges associated with implementing a operational cross-eye jammer are extreme [4], [6]–[11], [14]–[16], [19], [20], so it is only recently that practical systems have been demonstrated [17], [18], [21].

The main benefit of cross-eye jamming arises from the fact that a cross-eye jammer artificially recreates the worst case of the naturally-occurring phenomenon of glint which affects all types of radar. In recognition of this fact, cross-eye jamming is sometimes referred to as “artificial-glint jamming” (e.g. [16], [19]). Given that monopulse radars are affected by glint, they are also affected by cross-eye jamming.

The difficulties associated with implementing a cross-eye jammer relate to issues surrounding the worst-case glint angular error. The first problem is that the tolerances on the jammer system are extremely tight because the range of parameters over which large angular errors are induced is small [4], [6]–[9], [15], [16], [19], [20]. The second challenge arises because the worst-case glint angular error for two scatterers occurs when the returns from the scatterers have a phase difference of  $180^\circ$  and identical amplitudes. This relationship leads to cancellation of the signals leading to high Jammer-to-Signal Ratio (JSR) requirements, which imply high gain, power and isolation requirements [4], [6]–[11], [14]–[16], [19].

W. P. du Plessis, wduplessis@ieee.org, Tel: +27-12-841-3078, Fax: +27-12-841-2455.

This work was supported by the Armaments Corporation of South Africa (Armscor).

Despite the challenges associated with implementing cross-eye jamming, the development of a system which was used to perform sea trials [21] and the development of a range of systems which were demonstrated on operational platforms [17], [18] have been acknowledged. It thus appears that the required technologies have finally progressed to the point that operational cross-eye jammers are a realistic consideration.

Against this backdrop, research into cross-eye jamming was initiated at Defence, Peace, Safety and Security (DPSS), a division of the Council for Scientific and Industrial Research (CSIR), in 2007. While this work has been largely theoretical in nature, the focus has been on evaluating the implications of cross-eye jamming for operational systems. A number of important new conclusions relating to cross-eye jamming have been reached, and this paper aims to summarise these results and their significance.

Section II provides a brief review of cross-eye jamming, including a motivation for the retrodirective implementation. Section III summarises the results of an extended analysis of retrodirective cross-eye jamming with the emphasis on the implications of these results. Results considering the tolerances required from a cross-eye jammer are summarised in Section IV. The effect of platform skin return on the operation of a cross-eye jammer has also been evaluated and the main results are highlighted in Section V. A very brief description of the results obtained with a laboratory cross-eye jammer system is provided in Section VI, and the paper is concluded in Section VII.

## II. BRIEF REVIEW OF CROSS-EYE JAMMING

The most common explanation of cross-eye jamming is based on the phase-front analysis of glint [22]. The original reason for this is most likely due to the fact that the originators of the phase-front analysis of glint, Lewis (acknowledged in [22]) and Howard (author of [22]), are listed as co-inventors of one of the original cross-eye patents [2]. The continued popularity of the phase-front explanation is probably due to the graphical way the concept is explained.

Phase fronts are contours of equal phase, so all the points on a given phase front will correspond to the same phase of a signal. An example of the phase fronts generated by two sources is shown in Fig. 1. These phase-fronts move outwards from the sources over time, and are similar to ripples in a pond. In fact, reference [22] includes photographs of ripples in a water tank to demonstrate the principle.

The value of the phase-front analysis becomes clear with the observation that an antenna will receive the largest signal when it is aligned with the phase-fronts of a signal as shown in Fig. 2(a). A misalignment with the phase fronts as shown

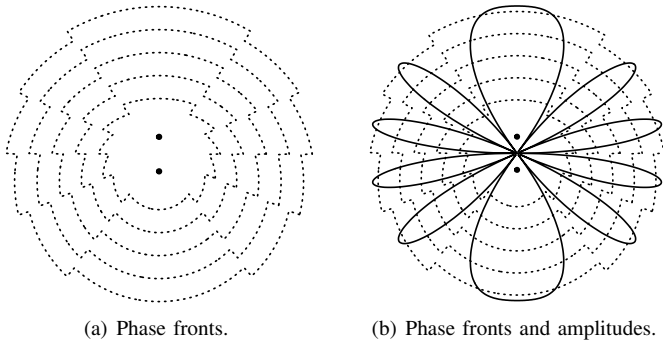


Fig. 1. The fields resulting from two sources of equal amplitude and 180° phase difference spaced 2.5 wavelengths apart [23].

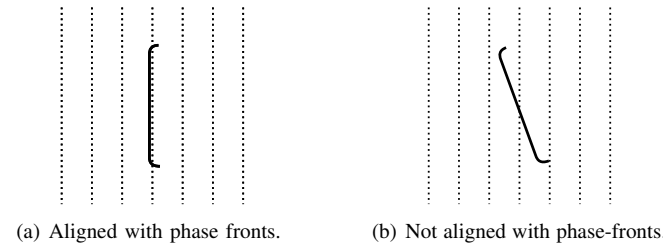


Fig. 2. Alignment of antenna aperture with phase fronts [23].

in Fig. 2(b) will lead to a lower signal because the signals from each portion of the antenna aperture will not add in phase. Importantly, this observation is true of any antenna.

The motivation for cross-eye jamming should now be clear from Fig. 1(a) because there are regions where an antenna aligned with the phase fronts will not point towards the sources of those phase fronts. These regions correspond to discontinuities in the phase-front patterns are extremely limited in angular extent. Fig. 1(a) shows that from most angles the system will act as a beacon which serves to assist threats in determining the position of the target rather than as a jammer. The limited angular extent over which large errors occur is the main reason for the extreme tolerance requirements on cross-eye jammers. For example, an error only 0.16 mrad in the estimated direction of a threat radar is sufficient to turn a perfect cross-eye jammer into a perfect beacon at 10 GHz with a 10-m jammer-antenna separation.

This extreme angular-positioning tolerance can be overcome using the retrodirective implementation of cross-eye jamming shown in Fig. 3. The concept of retrodirectivity is most easily understood by starting with a retrodirective array (often called a Van-Atta array after its inventor [24]) as shown in Fig. 3(a). The portion of the signal arriving at the top antenna will be received by the antenna, travel distances of  $l_1$ ,  $l_2$ ,  $l_3$  and  $l_4$  before being retransmitted by the bottom antenna. The portion of the signal arriving at the bottom antenna will follow the same path, but in the opposite direction. The signals transmitted by the two antennas will thus add in phase in the direction of the incoming signal, thereby causing the signal to be retransmitted back towards its source.

A retrodirective cross-eye jammer is identical in operation except that one of the directions through the system is shifted by 180° relative to the other direction. This causes a phase-front distortion to be retransmitted in the direction of the in-

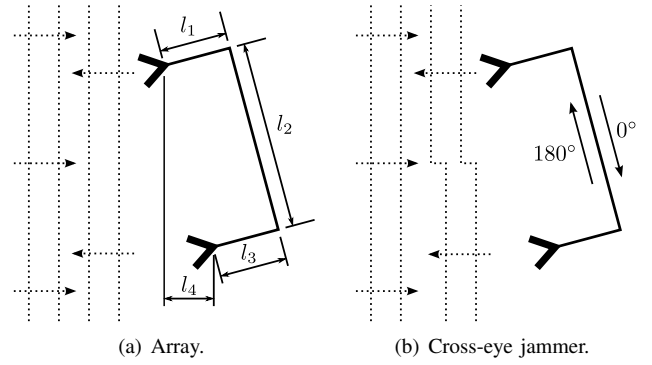


Fig. 3. Graphical description of the retrodirective concept [23].

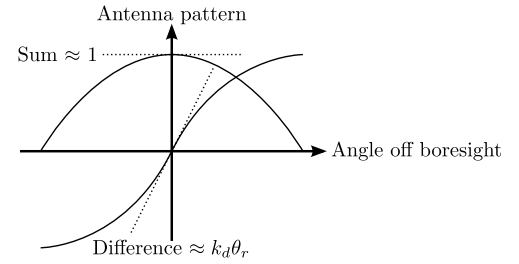


Fig. 4. Linearisation of monopulse antenna patterns (adapted from [23]).

coming signal as shown in Fig. 3(b). While the retrodirective implementation greatly eases the tolerance requirements on a cross-eye jammer, it does not completely remove them. The remaining tolerances arise because the required amplitude match and 180° phase shift implied in Fig. 3(b) must be accurately maintained for the jammer to be effective. Cross-eye tolerance requirements will be considered further in Section IV.

The origin of the requirement for high gain and power can be seen in Fig. 1(b) where a plot of the amplitude is placed over the phase-front plots. The amplitude match and 180° phase difference mean that the transmitted signals cancel in the direction of largest phase-front distortions. Extremely high JSR values are thus required for a cross-eye jammer to be effective, especially in the presence of platform skin return. This topic will be explored further in Section V.

Another extremely influential analysis of cross-eye jamming was presented by Vakin and Shustov [3]. The importance of this analysis lies in its relatively simple mathematical formulation and the fact that it is widely cited, usually via [4].

This analysis of cross-eye jamming is based on linear fits to the sum and difference-channel patterns of a monopulse radar as shown in Fig. 4. The total signal received by a monopulse radar's sum and difference channels will be

$$S_r = 1 + ae^{j\phi} \quad (1)$$

$$D_r = k_d (\theta_r + \theta_e) + ae^{j\phi} k_d (\theta_r - \theta_e) \quad (2)$$

$$= k_d [(1 + ae^{j\phi}) \theta_r + (1 - ae^{j\phi}) \theta_e] \quad (3)$$

where  $S_r$  and  $D_r$  are the sum- and difference-channel returns respectively,  $a$  and  $\phi$  are the relative amplitude and phase of the two jammer channels,  $k_d$  is defined in Fig. 4, and the remainder of the parameters are defined in Fig. 5.

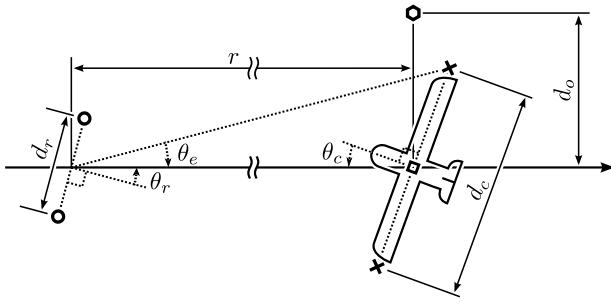


Fig. 5. Geometry of a cross-eye jamming scenario. The positions of the phase-comparison monopulse radar and cross-eye jammer antennas are denoted by circles and squares respectively. The position of the platform skin return and the apparent target are represented by a square and a hexagon respectively. (Adapted from [23], [25]–[29].)

The indicated angle is given by [10], [11], [15]

$$M = \Re \left\{ \frac{D_r}{S_r} \right\} \quad (4)$$

$$k_d \theta_i = \Re \left\{ \frac{k_d [(1 + ae^{j\phi}) \theta_r + (1 - ae^{j\phi}) \theta_e]}{1 + ae^{j\phi}} \right\} \quad (5)$$

$$\theta_i = \theta_r + \theta_e G_C \quad (6)$$

where  $M$  is the monopulse ratio,  $\theta_i$  is the monopulse indicated angle and  $G_C$  is the cross-eye gain given by [9]

$$G_C = \frac{1 - a^2}{1 + a^2 + 2a \cos(\phi)}. \quad (7)$$

The first important observation from (6) is that the indicated angle has two components. The first of these ( $\theta_r$ ) is simply the angle from boresight to the centre of the jammer and is dominant when the threat radar is unjammed. The second indicated-angle term ( $\theta_e G_C$ ) is a result of the operation of the jammer and can cause a large angular error.

The angular separation of the jammer antennas as seen by the radar ( $\theta_e$ ) is accurately approximated by [23]

$$\theta_e \approx \frac{d_c}{2r} \cos(\theta_c) \quad (8)$$

and increases as the jammer antenna separation ( $d_c$ ) increases and as the range ( $r$ ) decreases. While it is desirable to have as large a jammer-antenna separation as possible, practical considerations limit the maximum value to between 10 m and 20 m [21]. The fact that the indicated-angle error increases as range decreases ( $\theta_i \propto 1/r$ ) is the main motivation for the use of cross-eye jamming as a self-protection technique.

Noting that  $r \gg d_o$ , the indicated angle can be written as

$$\theta_i \approx \frac{d_o}{r}, \quad (9)$$

allowing the error induced by a cross-eye jammer (6) to be rewritten as

$$\frac{d_o}{r} \approx \frac{d_c}{2r} \cos(\theta_c) G_C \quad (10)$$

$$d_o \approx \frac{d_c}{2} \cos(\theta_c) G_C \quad (11)$$

where  $d_o$  is defined in Fig. 5. Equation (11) shows that the error induced by a cross-eye jammer is a fixed linear offset  $d_o$  rather than a fixed angular offset [9].

When the radar is pointing towards the centre of the jammer,  $\theta_r = 0$  allowing (6) to be rewritten as

$$G_C = \frac{\theta_i}{\theta_e} \quad (12)$$

showing that the cross-eye gain is the ratio of the angular error induced in the threat radar to  $\theta_e$ . When  $|G_C| = 1$ , the jammer return will appear to emanate from one of the jammer antennas, with the sign of  $G_C$  determining which jammer antenna. Values of  $|G_C| > 1$  will ensure that the apparent target is outside the physical extent of the jammer – the desired situation for a self-protection system. For example,  $|G_C| = 2$  means that  $\theta_i = 2\theta_e$ , so the radar will track a target  $\theta_e$  outside the jammer.

While these analyses of cross-eye jamming are useful and allow an understanding of cross-eye jamming to be gained, they suffer from two important limitations. Firstly, Vakin and Shustov [3] note that the assumptions inherent in the analysis leading to (6) and (7) mean that these results are only accurate when  $\theta_e/\theta_3 \leq 0.04$  to  $0.08$  and  $a \leq 0.9$  or  $a \geq 1.1$  where  $\theta_3$  is the sum-channel 3-dB beamwidth. Secondly, all the analyses described above make the assumption that the jammer acts only as a transmitter and the radar acts only as a receiver. This is clearly not true, and the retrodirective implementation of cross-eye jamming shown in Fig. 3(b) suggests that this assumption could lead to significant errors.

### III. EXTENDED ANALYSIS

The extended analysis described in [23], [25] was developed in an attempt to overcome the limitations of the analyses highlighted in Section II. The main benefits of the extended analysis are that it utilises nonlinear models of the antenna patterns and that it accounts for the retrodirective implementation of cross-eye jamming.

A phase-comparison monopulse system was used as the basis for the extended analysis [23], [25]. This approach has the benefit of directly modelling the most common monopulse implementation. However, more importantly, it has been shown that phase-comparison monopulse is an accurate model of any monopulse antenna pattern regardless of the implementation (e.g. amplitude-comparison, phased-array, etc.) [23]. The results of the extended analysis are thus applicable to any monopulse system and are not limited to phase-comparison monopulse.

The extended analysis proceeds in a similar manner to the derivation outlined in Section II, except that transmission from the radar to the jammer and the retrodirective implementation of the jammer are explicitly accounted for [23], [25].

The monopulse ratio is given by [23], [25]

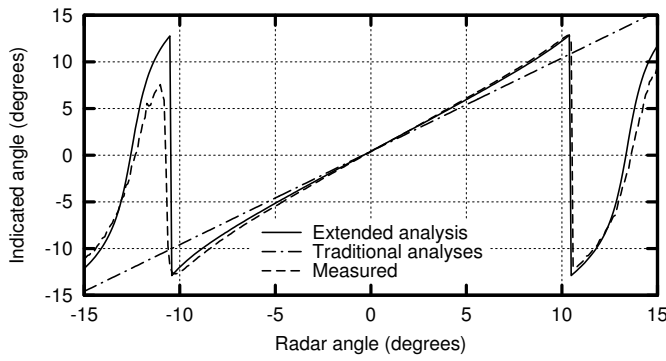
$$M_E = \frac{\sin(2k) + \sin(2k_c) G_C}{\cos(2k) + \cos(2k_c)} \quad (13)$$

where

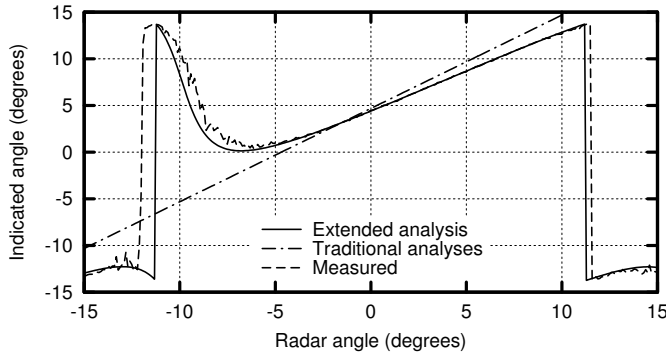
$$k \approx \beta \frac{d_r}{2} \sin(\theta_r), \quad (14)$$

$$k_c \approx \beta \frac{d_r}{2} \cos(\theta_r) \theta_e, \quad (15)$$

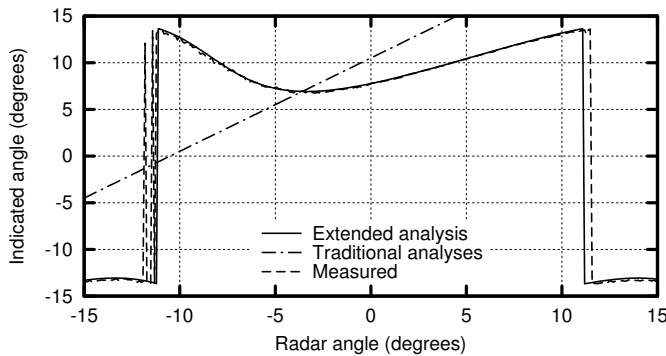
$M_E$  is the monopulse ratio,  $\beta$  is the free-space phase constant, and the approximations are extremely accurate for cross-eye jamming scenarios where  $\theta_e$  is small. The indicated angle



(a)  $a = -0.72$  dB and  $\phi = 120.1^\circ$  giving  $|G_C| = 0.16$ .



(b)  $a = -1.17$  dB and  $\phi = 200.4^\circ$  giving  $|G_C| = 1.9$ .



(c)  $a = -1.34$  dB and  $\phi = 192.9^\circ$  giving  $|G_C| = 4.2$ .

Fig. 6. Contours of constant angle factor [26] (© 2011 IEEE).

is computed from the monopulse ratio for phase-comparison monopulse [10], [11], [15]

$$M_E = \tan \left[ \beta \frac{d_r}{2} \sin(\theta_i) \right]. \quad (16)$$

It has been shown that the combination of (13) and (16) reduces to the same form as (6) under the conditions for which (6) is accurate [23].

The first important observation is that the forms of (6) and (13) are similar, each comprising two terms, one of which is related to the angle from boresight to the centre of the jammer and the other to the error induced by the cross-eye jammer. Furthermore, the jammer error term is related to  $\theta_e$  (through  $\sin(2k_c)$  in (13)) and the cross-eye gain, with the cross-eye gain acting as a scaling factor.

The theoretical results described above were validated through laboratory measurements conducted in the University of Pretoria's Compact Measurement range [23], [26].

A comparison between the theoretical and measured results is presented in Fig. 6 for a number of cases. In all cases the

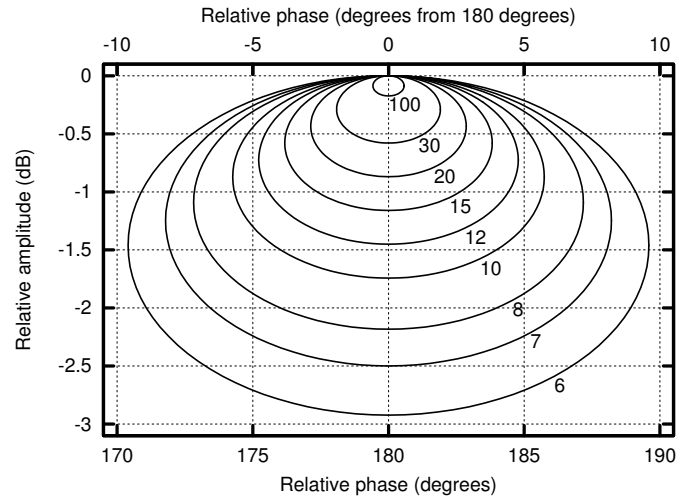


Fig. 7. Contours of constant cross-eye gain [27] (© 2011 IEEE).

agreement between the extended analysis and the measured results is excellent, thereby validating the extended analysis.

Fig. 6(a) shows a case where the jammer is extremely ineffective and for which (6) is accurate. As expected, the agreement between all three cases is excellent, except far from boresight, where the pattern nonlinearities become significant.

Fig. 6(b) demonstrates the effect of neglecting the non-linear nature of the monopulse antenna patterns in (6). The agreement between the three cases is again excellent near boresight, but the traditional analyses becomes increasingly inaccurate as the jammer moves away from boresight.

An extremely important observation about Fig. 6(b) is that the monopulse ratio never becomes zero at any angle. This means that the radar will not be able to track the target generated by the jammer and will simply rotate away from the jammer until lock is lost. In terms of (13), this situation arises when  $|\sin(2k_c) G_C| > 1$  because  $|\sin(2k)| \leq 1$ . This observation is extremely important as it was previously believed that a cross-eye jammer would only be able to generate targets inside the 3-dB beamwidth of the radar's sum channel (e.g. [3]–[6], [19], [30]). This apparent disagreement is explained by the fact that the traditional analyses of cross-eye jamming ignore both the nonlinear nature of the monopulse antenna patterns and the retrodirective implementation of the jammer.

Fig. 6(c) again demonstrates the inadequacies of the traditional analyses of cross-eye jamming, but for a case where the cross-eye gain is high. Here the traditional analysis fails to adequately predict the performance of the jammer, while the extended analysis agrees almost perfectly with the measurements.

#### IV. CROSS-EYE JAMMER SYSTEM TOLERANCES

The effect of tolerances on cross-eye jamming systems was evaluated by examining the relationship between the jammer parameters, and the cross-eye gain and the induced angular error [23], [27].

The relationship between the cross-eye gain and the amplitude and phase differences of the two jammer channels is described in Fig. 7 [23], [27]. Each contour shows the combination of jammer parameters which will achieve the specified cross-eye gain, with the specified gain being exceeded inside the relevant contour. The contours are mirrored around the

$a = 0$  dB curve [23], [27]. The centre of each constant-gain curve is at

$$a = \frac{G_C}{G_C + 1}, \phi = 180^\circ \quad (17)$$

so this combination of parameters should thus be used as a design goal to achieve a specified minimum cross-eye gain while allowing maximum parameter variations.

Importantly, Fig. 7 shows that it is possible to achieve values of cross-eye gain which place the apparent target well outside the physical extent of the jammer with surprisingly large parameter variations (e.g.  $|G_C| \geq 6$  requires  $a = -1.46 \text{ dB} \pm 1.46 \text{ dB}$  and  $\phi = 180^\circ \pm 9.56^\circ$ ).

The relationship between the induced angular error and the cross-eye gain for the extended analysis can be evaluated using [23], [27]

$$G_C \approx \frac{\sin[\beta d_r \sin(G_\theta \theta_e)]}{\sin(\beta d_r \theta_e)} \quad (18)$$

where  $G_\theta$  is the angle factor defined by

$$G_\theta = \frac{\theta_s}{\theta_e} \quad (19)$$

with  $\theta_s$  being the settling angle, which is defined as the angle where the monopulse ratio is zero. By (6) and (12), the angle factor is equal to the cross-eye gain for the traditional analyses of cross-eye jamming, so  $G_\theta$  has the same meaning in the extended analysis as  $G_C$  has in the traditional analyses.

Contours of constant angle factor are plotted in Fig. 8 [23], [27]. The first important observation is that the contours are larger than the corresponding curves in Fig. 7, suggesting that the allowable tolerances are wider than suggested by the traditional analyses. Furthermore, the contour sizes increase as the radar nears the jammer, showing that cross-eye jamming is even more effective at short ranges than traditionally believed.

Fig. 8 also demonstrates that there are conditions under which the monopulse ratio never becomes zero ( $G_\theta = \infty$ ), as noted previously in connection with Fig. 6(b). This condition occurs when the cross-eye gain satisfies [23], [27]

$$G_C \gtrsim \frac{\lambda}{\pi d_r} \times \frac{r}{d_c \cos(\theta_e)} \quad (20)$$

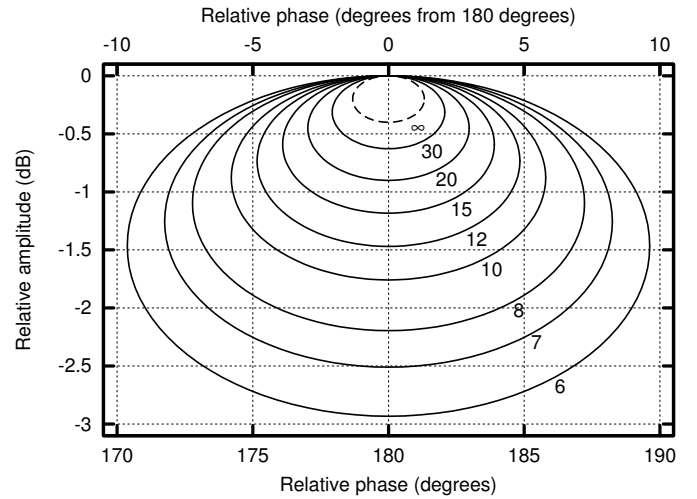
$$\gtrsim \frac{2}{\pi} \times \frac{\theta_3}{\theta_e} \quad (21)$$

where  $\theta_3$  is the radar sum-channel 3-dB beamwidth. As with the other gain contours, the size of this contour increases as the range decreases.

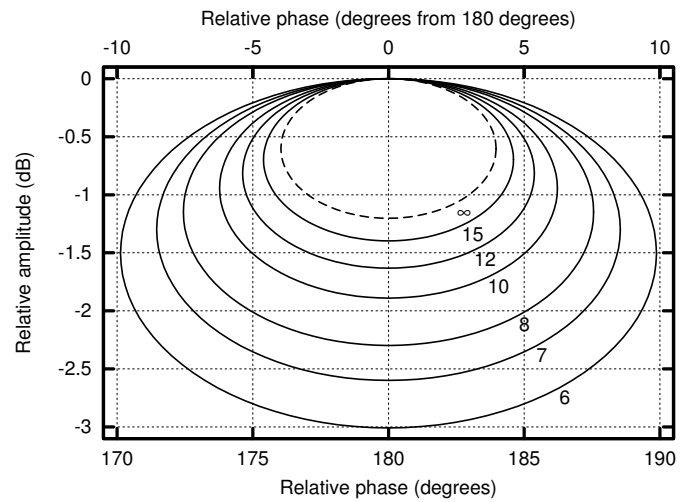
## V. INFLUENCE OF PLATFORM SKIN RETURN

The discussion above has focused on the performance of a cross-eye jammer in isolation. This case is important both because it allows the underlying properties of cross-eye jamming to be investigated and because it considers the scenario where a radar has been drawn off a platform's skin return before initiating cross-eye jamming. However, the timescales of modern engagements often do not allow sufficient time for a pull-off to be achieved before initiating cross-eye jamming. It is thus important to evaluate the effect of skin return on the performance of a cross-eye jammer.

Such an analysis was performed for retrodirective cross-eye jamming by including a point target halfway between



(a) Range of 10 km.



(b) Range of 1 km.

Fig. 8. Contours of constant angle factor [27] (© 2011 IEEE).

the jammer antennas as indicated by the square in Fig. 5 [28]. Surprisingly, the result of this analysis is identical to (13), except that the accurate approximation  $\cos(2k_c) \approx 1$  is required and the cross-eye gain becomes [28]

$$G_{Ct} = \Re \left\{ \frac{1 - ae^{j\phi}}{1 + ae^{j\phi} + a_s e^{j\phi_s}} \right\} \quad (22)$$

where  $a_s$  and  $\phi_s$  determine the amplitude and phase of the skin return respectively.

The fact that only the form of the cross-eye gain changes means that the results described above can be reused for the analysis of cross-eye jamming in the presence of skin return. Importantly, the relationships in Section IV can be reused by simply computing the cross-eye gain with (22) instead of (7).

The JSR of a cross-eye jammer is defined as the ratio of stronger of the two jammer signals to the skin return [6], [9], so the relationship between  $a_s$  and JSR is [28]

$$\text{JSR} = \frac{1}{a_s^2}. \quad (23)$$

The Radar Cross Section (RCS) is an important property of military platforms and is thus well characterised, at least in maximum-value terms. However, the phase of skin return at any moment inherently cannot be accurately controlled or

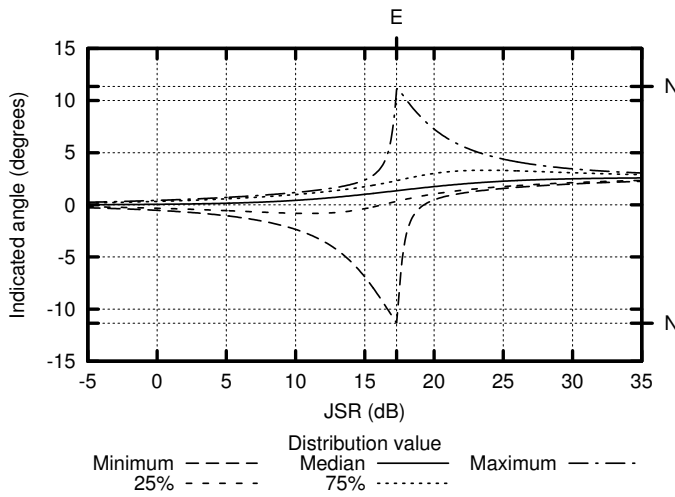


Fig. 9. A plot showing the indicated angle variation as a function of JSR for the scenario described in the text [28] (© 2011 IEEE).

predicted because full knowledge of the position of every portion of the target would be required. The indicated angle is thus a distribution rather than a single value because  $\phi_s$  can have any phase value with equal probability [28].

Fig. 9 shows the indicated angle seen by an X-Band radar with a  $10^\circ$  beamwidth which is 1 km away from a cross-eye jammer with a 10-m jammer-antenna separation and a  $30^\circ$  rotation [23], [25], [28]. The curves labelled “25%” and “75%” show that the specified proportion of the indicated angles will be below these curves (the minimum, median and maximum curves would be labelled “0%,” “50%” and “100%” respectively under this scheme). The first nulls of the sum-channel antenna pattern are indicated by “N” on the right axis.

The indicated angles in Fig. 9 vary from the position of the skin return ( $0^\circ$ ) to the position of the cross-eye jammer return ( $3.1^\circ$ ) as the JSR increases. This behaviour is anticipated because the skin return will dominate at low JSR, while the jammer will dominate at high JSR.

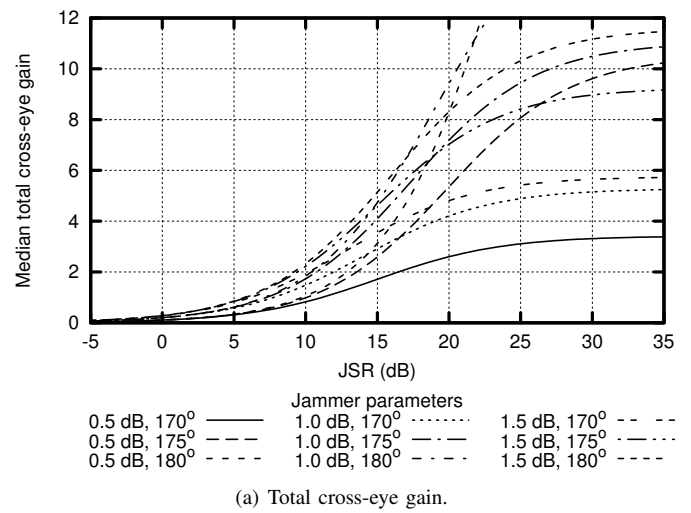
The median indicated angle increases monotonically, and the central 50% of the distribution (bounded by the curves labelled “25%” and “75%”) displays relatively small variations as the JSR increases. However, the extreme values display large variations, and can even stretch to the edges of the sum-channel antenna beam.

This large variation occurs when the skin return has a similar magnitude to the cross-eye jammer return. The JSR value where these two values are equal is indicated by “E” on the top axis of Fig. 9 and corresponds to the JSR with the largest indicated-angle variation. The total sum-channel return at this critical JSR value can be zero, leading to an infinite monopulse ratio in (13) which will place the apparent target at the edge of the sum-channel beam by (16).

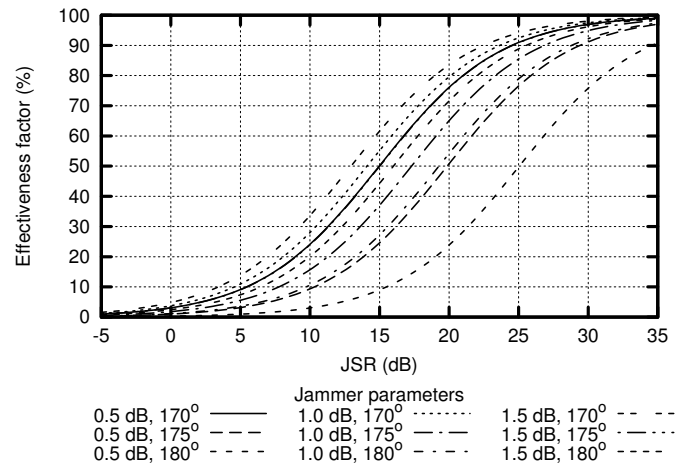
The median total cross-eye gain in the presence of skin return is a useful figure of merit because a tracking filter will tend to track near the median of a distribution. The median total cross-eye gain is given by [28]

$$G_{Ctm} = \frac{1 - a^2}{1 + a^2 + 2a \cos(\phi) + a_s^2} \quad (24)$$

$$= G_C \cdot K_S \quad (25)$$



(a) Total cross-eye gain.



(b) Effectiveness factor. Note that the 0.5 dB,  $170^\circ$  and 1.5 dB,  $175^\circ$  plots are almost identical.

Fig. 10. The median cross-eye gain in the presence of skin return [28] (© 2011 IEEE).

where

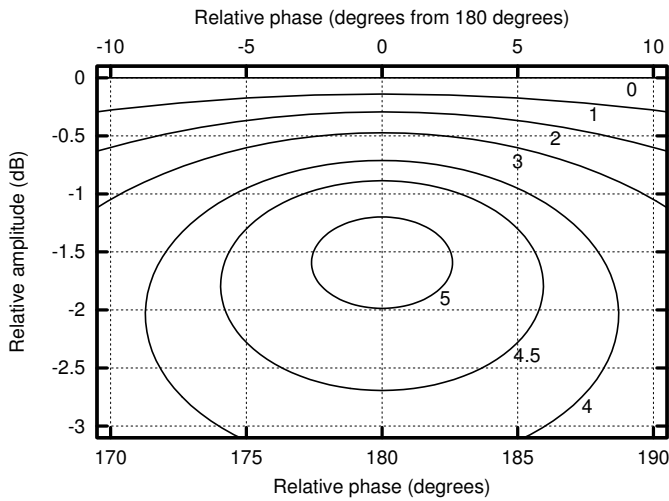
$$K_S = \frac{1 + a^2 + 2a \cos(\phi)}{1 + a^2 + 2a \cos(\phi) + a_s^2} \quad (26)$$

is an effectiveness factor. The median total cross-eye gain in the presence of skin return is thus the product of the cross-eye gain for an isolated jammer (7) and  $K_C$  which depends on the jammer return and the skin return.

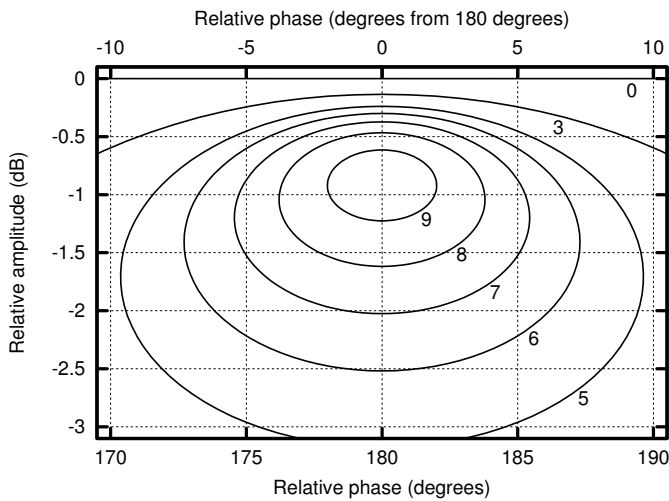
Fig. 10 shows  $G_{Ctm}$  and  $K_C$  as a function of JSR. There is a compromise between choosing the jammer parameters to achieve high  $G_C$  and choosing the jammer parameters for high  $K_C$ . For example, the highest  $G_C$  in Fig. 10(a) is achieved by the 0.5 dB,  $180^\circ$  case, but this case also has the lowest  $K_C$  in Fig. 10(b). Fig. 10(a) shows that this case has a lower  $G_{Ctm}$  than the 1.5 dB,  $170^\circ$  case until the JSR is higher than 15 dB due to the latter case’s higher  $K_C$ .

However, the most important observation from Fig. 10(a) is that median indicated angles outside the physical extent of a cross-eye jammer are possible in all cases considered for JSR values of 15 dB, and in most cases considered for JSR values of only 10 dB. These values are in contrast to the widely-stated view that 20-dB JSR is required for effective cross-eye jamming (e.g. [7]–[9], [16]).

Fig. 11 shows constant  $G_{Ctm}$  contours in the presence of skin return for two JSR values. These curves are for the same



(a) JSR is 15 dB.



(b) JSR is 20 dB.

Fig. 11. Contours of constant median total cross-eye gain in the presence of skin return [28] (© 2011 IEEE).

conditions as those in Figs 7 and 8(a), and the effect of skin return can be clearly seen.

The first effect is that the achievable median total cross-eye gain values are significantly decreased by the presence of skin return. This is anticipated as the skin return will tend to counteract the effect of cross-eye jamming. However, angle factors large enough to generate a target outside the physical extent of the jammer ( $|G_\theta| > 1$ ) are still possible with reasonable tolerances even with a JSR of only 15 dB.

The second effect is that the contours no longer all pass through the point  $a = 0$  dB,  $\phi = 180^\circ$ . This is a result of the fact that the  $K_C$  is lower in this region because the cross-eye signals are more closely matched leading to greater jammer-signal cancellation. The value of  $K_C$  increases as one moves away from this point, leading to better agreement with Figs 7 and 8(a).

Another extremely surprising result is that the optimal design point in the presence of skin return is identical to that for an isolated cross-eye jammer in (17), except that that  $G_{Ctm}$  should be used instead of  $G_C$  [28]. This result means that the design point for a cross-eye jammer does not depend on the presence or absence of skin return or on the JSR.

The parameter relationships to ensure that all possible

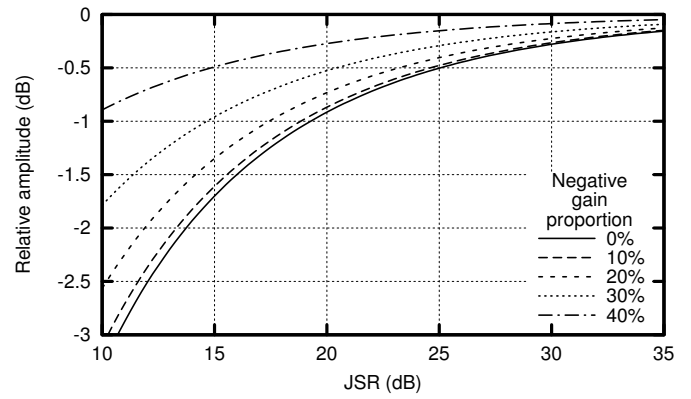


Fig. 12. The relationship between the jammer transmitter amplitudes and the JSR required to limit the proportion of indicated angles on the wrong side of the jammer to a specified value [29] (© 2012 IEEE).

indicated angles are limited to one side of a cross-eye jammer can be useful. This condition occurs when [29]

$$JSR \gtrsim (1 - a)^{-2} \quad (27)$$

where the approximation is accurate when  $\phi \approx 180^\circ$ .

The relationship between  $a$  and the JSR to ensure that only a specified proportion of the possible indicated angles are on the opposite side of the jammer to the desired apparent target has also been investigated, and the results are summarised in Fig. 12 [29]. The proportion of possible indicated angles on the wrong side of the jammer will be limited to the specified value when the combination of parameters is below and to the right of the relevant curve in Fig. 12.

## VI. LABORATORY CROSS-EYE DEMONSTRATOR

A simple laboratory cross-eye jammer demonstrator was constructed at the CSIR early in 2010 and was successfully demonstrated against a monopulse radar.

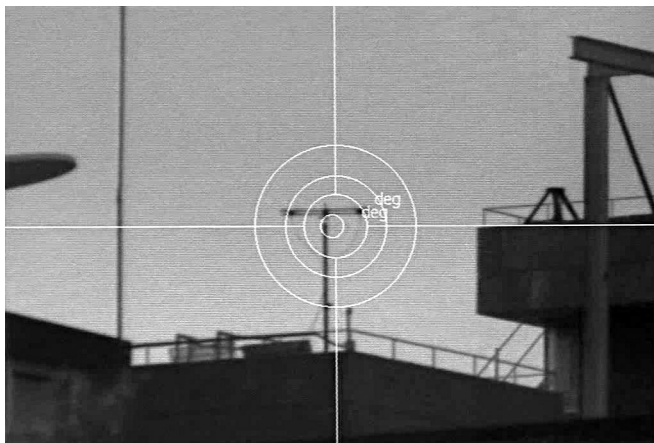
The system was based on two locally-developed digital radio-frequency memory (DRFM) boards [31] with modified firmware. A combination of prototype Radio Frequency (RF) hardware and portions of an older DRFM system were used to amplify, split, combine, filter and mix the signals.

The results obtained against a monopulse radar are shown in Fig. 13. The test started with the radar pointing towards the centre of the jammer as shown in Fig. 13(a) with the radar's tracking disabled. Radar tracking was then enabled, and the radar rapidly moved to track an apparent target well outside the physical extent of the jammer antennas as shown in Fig. 13(b).

While this demonstrator suffered from a number of limitations, the results obtained are nonetheless significant. A large angular error was induced in a monopulse radar despite the use of a combination of prototype, laboratory and older hardware, and even though only two weeks were available in which to complete the work. Achieving this positive result while overcoming these extreme challenges suggests that constructing a cross-eye jammer is not as complex as is widely believed.

## VII. CONCLUSION

Roughly sixty years after the idea of cross-eye jamming was first proposed, it appears that technology has finally



(a) Radar pointed towards jammer.



(b) Radar tracking activated.

Fig. 13. Demonstration of the effect of the cross-eye jamming demonstrator. The jammer antennas are the dark patches at the ends of the cross-bar of the T-shaped stand.

matured to the level required to implement operational cross-eye jammers. Research into cross-eye jamming was initiated at the CSIR as a result of this observation, and the main results are summarised above.

Important considerations from an operational perspective include:

- the retrodirective implementation appears to be the only practical implementation of cross-eye jamming,
- ignoring the retrodirective implementation means that significant errors exist in the traditional analyses of cross-eye jamming,
- a retrodirective cross-eye jammer can break a monopulse radar lock,
- the tolerance requirements on a cross-eye jammer have been quantified and appear less strict than was previously believed, and
- the widely-quoted JSR requirement of 20 dB for effective cross-eye jamming, though realistic, is conservative.

Taken together, these observations suggest that retrodirective cross-eye jamming is a viable alternative for platform self-protection against radar-guided threats. The fact that a laboratory cross-eye jammer could be constructed and demonstrated against a monopulse radar despite extreme challenges serves to support this observation.

## ACKNOWLEDGMENT

The author wishes to express his sincere thanks to Klasic Olivier and Anneli Kew for their assistance in constructing the laboratory cross-eye demonstrator described herein.

## REFERENCES

- [1] P. K. Shizume, "Angular deception countermeasure system," U.S.A. Patent 4 117 484, September 26, 1978.
- [2] B. L. Lewis and D. D. Howard, "Security device," U.S.A. Patent 4 006 478, February 1, 1977.
- [3] S. A. Vakin and L. N. Shustov, "Principles of jamming and electronic reconnaissance - volume I," U.S. Air Force, Tech. Rep. FTD-MT-24-115-69, AD692642, 1969.
- [4] L. B. Van Brunt, *Applied ECM*. EW Engineering, Inc., 1978, vol. 1.
- [5] A. Golden, *Radar Electronic Warfare*. AIAA Inc., 1987.
- [6] R. N. Lothes, M. B. Szymanski, and R. G. Wiley, *Radar vulnerability to jamming*. Artech House, 1990.
- [7] D. C. Schleher, *Electronic warfare in the information age*. Artech House, 1999.
- [8] D. L. Adamy, *EW 101: A first course in electronic warfare*. Artech House, 2001.
- [9] F. Neri, *Introduction to Electronic Defense Systems*, 2nd ed. SciTech Publishing, 2006.
- [10] A. I. Leonov and K. I. Fomichev, "Monopulse radar," U.S. Air Force, Tech. Rep. FTD-MT-24-982-71, AD742696, 1972.
- [11] A. I. Leonov and K. I. Fomichev, *Monopulse radar*. Artech House, 1986.
- [12] D. K. Barton, *Modern radar system analysis*. Artech House, 1988.
- [13] G. W. Stimson, *Introduction to airborne radar*, 2nd ed. SciTech Publishing, 1998.
- [14] A. Farina, "Electronic counter-countermeasures," in *Radar Handbook*, 3rd ed., M. I. Skolnik, Ed. McGraw-Hill, 2008, ch. 24.
- [15] S. M. Sherman and D. K. Barton, *Monopulse Principles and Techniques*, 2nd ed. Artech House, 2011.
- [16] G. E. Johnson, "Jamming passive lobing radars," *Electronic Warfare*, vol. 9, pp. 75-85, April 1977.
- [17] F. Neri, "Experimental testing on cross-eye jamming," in *AOC Conference*, 2000.
- [18] F. Neri, "Anti-monopulse jamming techniques," in *Proc. 2001 SBMO/IEEE MTT-S Microwave and Optoelectronics Conf.*, vol. 2, 2001, pp. 45-50.
- [19] P. E. Redmill, "The principles of artificial glint jamming ("cross eye")," Royal Aircraft Establishment (Farnborough), Tech. note RAD. 831, March 1963.
- [20] D. C. Jenn. (2011, March) Microwave devices & radar lecture notes volume IV. Naval Postgraduate School. Ver. 6.0. [Online]. Available: <http://www.dcjenn.com/EC4610/VoIIVv6.0.pdf>
- [21] L. Falk, "Cross-eye jamming of monopulse radar," in *IEEE Waveform Diversity & Design Conf.*, 4-8 June 2007, pp. 209-213.
- [22] D. D. Howard, "Radar target angular scintillation in tracking and guidance systems based on echo signal phase front distortion," in *Proc. Nat. Eng. Conf.*, vol. 15, 1959, reprinted in *Radars*, Vol. 4, Radar Resolution & Multipath Effects, David K. Barton, Ed., Artech House, 1975.
- [23] W. P. du Plessis, "A comprehensive investigation of retrodirective cross-eye jamming," Ph.D. dissertation, University of Pretoria, 2010.
- [24] L. C. Van Atta, "Electromagnetic reflector," U.S.A. Patent 2 908 002, Oct. 6, 1959.
- [25] W. P. du Plessis, J. W. Odendaal, and J. Joubert, "Extended analysis of retrodirective cross-eye jamming," *IEEE Trans. Antennas Propag.*, vol. 57, no. 9, pp. 2803-2806, September 2009.
- [26] W. P. du Plessis, J. W. Odendaal, and J. Joubert, "Experimental simulation of retrodirective cross-eye jamming," *IEEE Trans. Aerosp. Electron. Syst.*, vol. 47, no. 1, pp. 734-740, January 2011.
- [27] W. P. du Plessis, J. W. Odendaal, and J. Joubert, "Tolerance analysis of cross-eye jamming systems," *IEEE Trans. Aerosp. Electron. Syst.*, vol. 47, no. 1, pp. 740-745, January 2011.
- [28] W. P. du Plessis, "Platform skin return and retrodirective cross-eye jamming," *IEEE Trans. Aerosp. Electron. Syst.*, vol. 48, no. 1, pp. 490-501, January 2012.
- [29] W. P. du Plessis, "Limiting apparent target position in skin-return influenced cross-eye jamming," *IEEE Trans. Aerosp. Electron. Syst.*, updated version submitted 25 May 2012, under review.
- [30] T. W. Tucker and B. Vidger, "Cross-eye jamming effectiveness," Tactical Technologies Inc., Ottawa, ON K2A 3V6, Tech. Rep., 2009.
- [31] K. Olivier, J. E. Cilliers, and M. du Plessis, "Design and performance of wideband DRFM for radar test and evaluation," *Electron. Lett.*, vol. 47, no. 14, pp. 824-825, 7 July 2011.